# Microwave Characteristics of a Pseudomorphic High Electron Mobility Transistor under Electro-Optical Stimulations

D. M. Kim, *Member, IEEE,* S. H. Song, *Member, IEEE,* K. H. Baek, *Student Member, IEEE,* D. J. Kim, *Member, IEEE,* and H. J. Kim

***Abstract*—Comprehensive $P_{\rm opt}$-, $V_{\rm GS}$-, and $V_{\rm DS}$-dependent variations of microwave performances ($f_T$ and $f_{\rm max}$) in a PHEMT under electro-optical stimulation are reported for the first time. Under low $P_{\rm opt}$, microwave characteristics are observed to be predominantly modulated by the photoconductive effect through the transconductance. Under high optical power, however, they are limited by the photovoltaic effect through the gate capacitance and a parasitic MESFET activated parallel to the $In_{0.13}Ga_{0.87}As$ channel PHEMT. Contrary to the dc current-voltage (*I–V*) characteristics, which are predominantly controlled by the photoconductive effect with a strong nonlinearity due to a parallel conduction, microwave characteristics strongly depend on the photovoltaic effect as well as the photoconductive effect under electro-optical stimulation. An extended small-signal photonic-microwave model is suggested for better description of PHEMT's under electro-optical stimulations.**

***Index Terms*—Cut-off frequency, HEMT, microwave, photonics, optical control.**

## I. Introduction

CONSIDERING microwave-photonics as a promising vehicle for high-speed and high-capacity communication systems, a pseudomorphic high electron mobility transistor (PHEMT) is one of the most competing devices for high performance photonic-microwave circuits and systems due to its superior electro-optical performances [1]–[8]. We also expect that variations of photonic-dc/microwave characteristics in PHEMT's under electro-optical co-stimulation can be used as an extended nondestructive characterization technique for physical mechanisms in the failure and degradation of heterostructure field effect transistors [9].

In this work, photonic-microwave characteristics of an n-channel $Al_{0.3}Ga_{0.7}As/GaAs/In_{0.13}Ga_{0.87}As$ PHEMT are reported for possible applications both as a photonic-microwave responsive device and as a novel method for the characterization of traps-related mechanisms in PHEMT's with multiple hetero-interface epitaxial structures. The current gain cut-off frequency $(f_T)$ and the maximum frequency of oscillation $(f_{\rm max(MAG)})$ have been characterized for various electrical operating conditions and optical powers over $P_{\rm opt} = 0 \sim 30$ mW with $\lambda = 0.83\ \mu$m. Physical mechanisms involved in the variation of photonic microwave characteristics are analytically explained and an extended photonic-microwave equivalent circuit model is suggested for better description of microwave performances of PHEMT's under electro-optical stimulation.

Manuscript received September 15, 1999; revised October 22, 1999. This work was supported by KOSEF under the ERC program through the MINT Research Center, Dongguk University, and in part by the Grant 981-0908-029-2 from the Basic Research Program. The review of this paper was arranged by Editor H.-H. Vuong.

D. M. Kim, K. H. Baek, and D. J. Kim are with the School of Electrical Engineering, Kookmin University, Seoul 136-702, Korea (e-mail: dmkim@kmu.kookmin.ac.kr).

S. H. Song is with Samsung Electronics, Kyungki 449-900, Korea.

H. J. Kim is with the Photonics Research Center, Korea Institute of Science and Technology, Seoul 130-760, Korea.

Publisher Item Identifier S 0741-3106(00)02117-0.

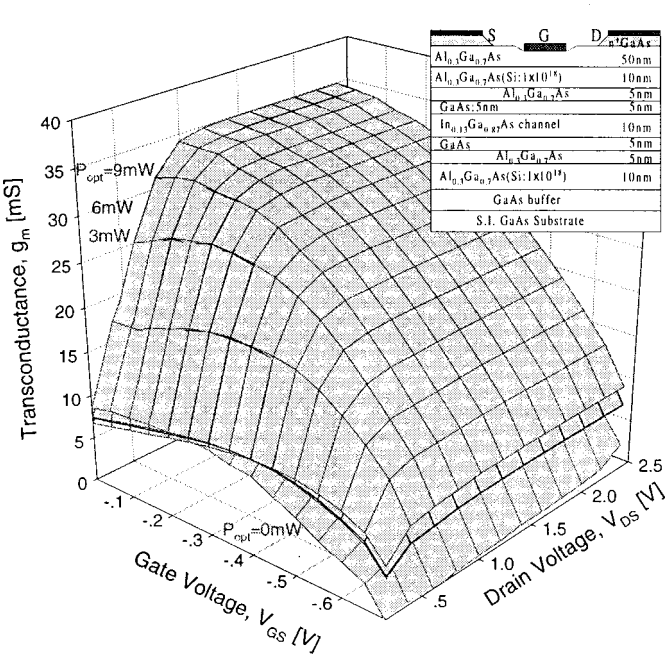


Fig. 1. Transconductance characteristics of a PHEMT (a V-shaped gate with $L_g = 1\ \mu$m, $L_{\rm gd} = L_{\rm gs} = 1\ \mu$m, and $W = 2 \times 100\ \mu$m as in the inset) under electro-optical stimulations ($P_{\rm opt} = 0$, 3, 6, and 9 mW).

## II. Microwave Characteristics of a PHEMT under Electro-Optical Stimulation

An n-channel $Al_{0.3}Ga_{0.7}As/GaAs/In_{0.13}Ga_{0.87}As$ PHEMT, which has a V-shaped gate with $L_g = 1\ \mu$m, $W = 2 \times 100\ \mu$m, $L_{\rm gs} = L_{\rm gd} = 1\ \mu$m as shown in Fig. 1, was used for an investigation of photonic-microwave characteristics under electro-optical stimulations [10]. Transconductance $(g_m = \partial I_d / \partial V_{\rm gs})$ characteristics are also shown in Fig. 1 for optical powers $P_{\rm opt} = 0 \sim 30$ mW. Electro-optical effects on the drain current $(I_D)$ and the transconductance, are saturated

TABLE I
HIGHEST VALUES OF CURRENT GAIN CUT-OFF FREQUENCY ($f_{T|\max}$), MAXIMUM FREQUENCIES OF OSCILLATION ($f_{\max(\mathrm{MAG})|\max}$ AND $f_{\max(U)|\max}$) UNDER ELECTRO-OPTICAL STIMULATIONS ($P_{\mathrm{opt}} = 0, 3, 20,$ AND 30 mW) WITH BIAS CONDITIONS ($V_{\mathrm{GS}}$ and $V_{\mathrm{DS}}$).

| $P_{opt}$ | $f_{T\|\max}(V_{GS},V_{DS})$ | $f_{max(MAG)\|\max}(V_{GS},V_{DS})$ | $f_{max(U)\|\max}(V_{GS},V_{DS})$ |
|---|---|---|---|
| 0mW | 6.62GHz (0.0,2.4V) | 16.89GHz (0.0,2.4V) | 3.32GHz (-0.7,2.4V) |
| 3mW | 9.31GHz (0.0,1.4V) | 31.45GHz (0.0,2.4V) | 4.40GHz (-0.7,1.4V) |
| 20mW | 10.95GHz (0.0,1.4V) | 41.79GHz (0.0,2.4V) | 4.88GHz (-0.7,1.4V) |
| 30mW | 11.02GHz (-0.1,1.4V) | 57.15GHz (0.0,2.4V) | 4.86GHz (-0.7,1.4V) |

predominantly due to a parallel conduction under high optical stimulation [11]. Microwave characteristics are measured as a function of the gate voltage ($V_{\mathrm{GS}}$), the drain voltage ($V_{\mathrm{DS}}$), and the optical power ($P_{\mathrm{opt}}$). $P_{\mathrm{opt}}$-dependent $f_T$ and $f_{\max(\mathrm{MAG})}$ have been investigated from scattering parameters measured by an HP-8510B vector network analyzer.

Under electro-optical stimulations, photonic-microwave characteristics are measured and bias-dependent maximum values of $f_T$ and $f_{\max(\mathrm{MAG})}$ are obtained as summarized in Table I. Without optical illumination ($P_{\mathrm{opt}} = 0$), maximum values of $f_T$ and $f_{\max(\mathrm{MAG})}$ were measured to be 6.62 GHz and 16.89 GHz, respectively. As expected, they depend strongly on both $V_{\mathrm{GS}}$ and $V_{\mathrm{DS}}$, primarily due to the modulation of transconductance, parasitic capacitances, and parasitic resistances under electro-optical stimulation. Highest values of $f_T$ and $f_{\max(\mathrm{MAG})}$ under $P_{\mathrm{opt}} = 30$ mW were improved to $f_T = 11.02$ GHz and $f_{\max(\mathrm{MAG})} = 57.15$ GHz, respectively. Compared with relatively small change from $f_T = 6.62$ to 11.02 GHz, we observed a significant improvement in $f_{\max(\mathrm{MAG})}$ from 16.89 to 57.15 GHz under $P_{\mathrm{opt}} = 30$ mW. Highest values of both $f_T$ and $f_{\max(\mathrm{MAG})}$ were observed at large $V_{\mathrm{DS}}$ and zero gate voltage, which has both a high channel carrier density and a high channel electric field with a small gate capacitance. We also observed sharp increase in $f_{\max(\mathrm{MAG})}$ while saturated $f_T$ with increasing optical power for a specific electrical bias $V_{\mathrm{GS}}$ and $V_{\mathrm{DS}}$.

Under optical stimulation, predominant characteristic parameters in the variation of both dc and microwave characteristics of PHEMT's include the transconductance, which is modulated mainly by *the photoconductive effect* due to increased channel carrier concentration, and parasitic capacitances, which are controlled predominantly by *the photovoltaic effect*, at a specific electrical bias. Based on a conventional small-signal model of PHEMT's with $R_{\mathrm{sd}}$ as a total source-drain resistance ($R_{\mathrm{sd}} = R_s + R_d$), the current gain cut-off frequency is described by [12]

$$f_T = \frac{g_m}{2\pi} \cdot \frac{1}{(C_{\mathrm{gs}} + C_{\mathrm{gd}}) \cdot [1 + g_{\mathrm{ds}} R_{\mathrm{sd}}] + g_m C_{\mathrm{gd}} R_{\mathrm{sd}}} \quad (1)$$

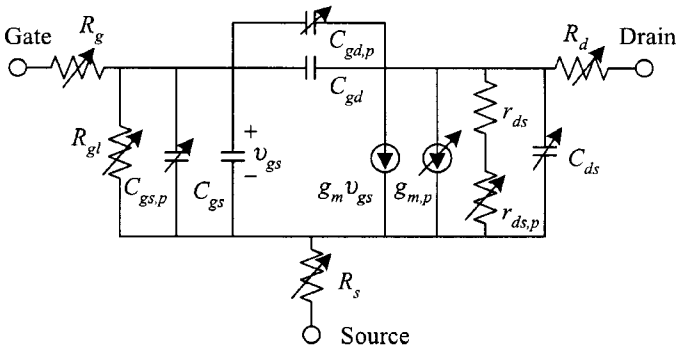


Fig. 2. Extended photonic-microwave equivalent circuit including optically induced transconductance ($g_{m,p}$), gate capacitances ($C_{\mathrm{gs},p}, C_{\mathrm{gd},p}$), output resistance enhancement $r_{\mathrm{ds},p}$, and gate leakage as a parallel resistor ($R_{\mathrm{gl}}$) under electro-optical stimulations.

where the gate capacitance ($C_g = WL\varepsilon_{\mathrm{eff}}/d_{\mathrm{eff}}$) and $g_m$ depend strongly on electro-optical stimulations ($P_{\mathrm{opt}}, V_{\mathrm{GS}}$ and $V_{\mathrm{DS}}$) as well as the epitaxial structure of the PHEMT under characterization.

The maximum frequency of oscillation ($f_{\max(\mathrm{MAG})}$) can also be described by (2), shown at the bottom of the page [13], where $g_{\mathrm{ds}}$, $C_{\mathrm{gs}}(C_{\mathrm{gd}})$, $R_{\mathrm{ch}}$, and $R_g(R_s)$ mean the output conductance, the gate-source(-drain) capacitance, intrinsic channel resistance, and parasitic gate(source) resistance, respectively. As expected, $f_{\max(\mathrm{MAG})}$ depends strongly on parasitic resistances and capacitances as well as $g_m$ via $f_T$ and depends strongly on $P_{\mathrm{opt}}$.

Considering variations of characteristic parameters under optical stimulation, an extended photonic-microwave equivalent circuit model is proposed in Fig. 2. In addition to electrically controlled characteristic model parameters ($g_m, C_{\mathrm{gs}}, C_{\mathrm{gd}}, r_{\mathrm{ds}}$) and parasitic resistances ($R_g, R_d, R_s$), we included $P_{\mathrm{opt}}$-dependent model parameters ($g_{m,p}, C_{\mathrm{gs},p}, C_{\mathrm{gd},p}, r_{\mathrm{ds},p}$, and $g_{\mathrm{gl}} = 1/R_{\mathrm{gl}}$) for better description of photonic-microwave characteristics of PHEMT's. As experimentally described in the small-signal model parameters for $P_{\mathrm{opt}} = 20$ mW in [5], gate capacitances ($C_{\mathrm{gs}}, C_{\mathrm{gd}}$) and output resistance $r_{\mathrm{ds}}$ ($1/r_{\mathrm{ds}} = g_{\mathrm{ds}} = dI_d/dV_{\mathrm{ds}}$), as well as transconductance, increase with $P_{\mathrm{opt}}$ while parasitic resistances ($R_g, R_s, R_d$) decrease due to optically generated excess carriers. This extended photonic-microwave model agrees well with experimental observation in PHEMT's under optical stimulation. Under electro-optical stimulation, the optically induced photoconductivity and the photovoltage ($V_{\mathrm{opt}} = V_{P(0\ \mathrm{mW})} - V_P$, $V_P$ = pinch-off voltage) are dominant parameters in the modulation of photonic-microwave characteristics. The photoconductive effect, due to optically stimulated excess channel carriers above electrically induced channel carriers controlled by $V_{\mathrm{GS}}$, appears predominantly on the parasitic resistances and transconductance ($g_m = g_{\mathrm{mo}} + g_{\mathrm{mp}}$) which is saturated at high

$$f_{\max(\mathrm{MAG})} = \frac{f_T}{\sqrt{4g_{\mathrm{ds}}\left(R_{\mathrm{ch}} + \frac{R_s + R_g}{1 + g_m R_s}\right) + \frac{4}{5} \cdot \frac{C_{\mathrm{gd}}}{C_{\mathrm{gs}} + C_{\mathrm{gd}}} \cdot \left(1 + \frac{5}{2}\frac{C_{\mathrm{gd}}}{C_{\mathrm{gs}} + C_{\mathrm{gd}}}\right) \cdot (1 + g_m R_s)^2}} \quad (2)$$

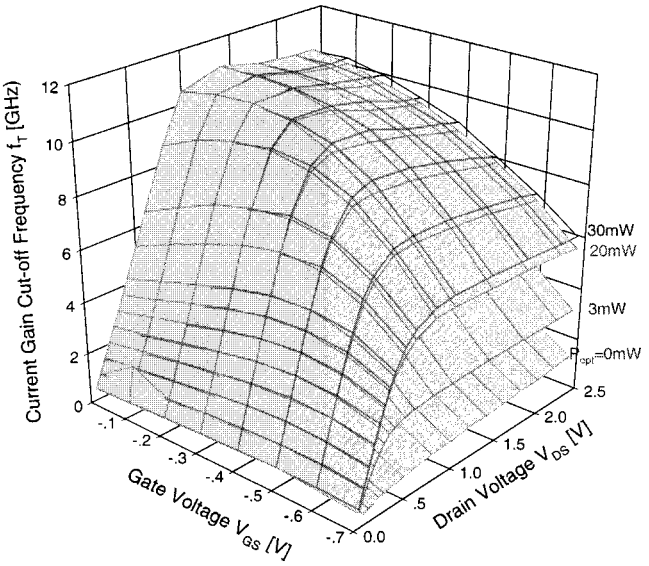


Fig. 3. Current gain cut-off frequencies ($f_T$'s) of a PHEMT as a function of $V_{\rm DS}$ and $V_{\rm GS}$ under electro-optical stimulations ($P_{\rm opt} = 0, 3, 20,$ and 30 mW).

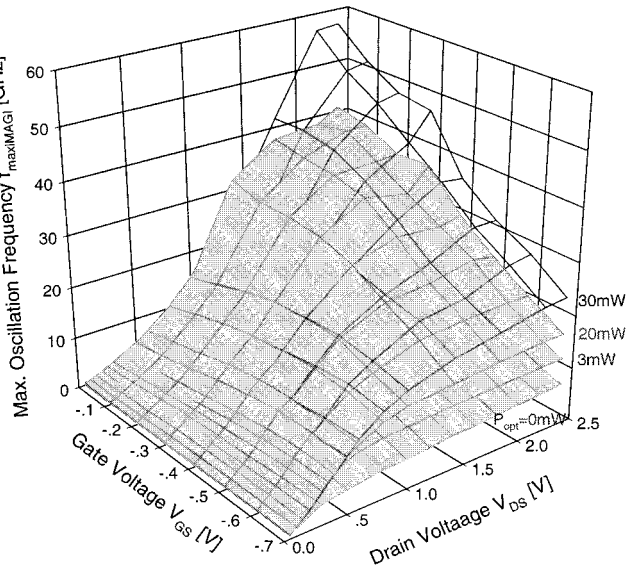


Fig. 4. Maximum oscillation frequencies ($f_{\max(\rm MAG)}$'s) of a PHEMT as a function of $V_{\rm DS}$ and $V_{\rm GS}$ under electro-optical stimulations ($P_{\rm opt} = 0, 3, 20,$ and 30 mW).

$P_{\rm opt}$ (>3 mW) as explicitly shown in Fig. 1. $P_{\rm opt}$-dependent transconductance can be modeled with $g_{\rm mo}$ (transconductance under $P_{\rm opt} = 0$) and proportionality constants ($a$, $b$, and $a'$) as (3), shown at the bottom of the page, where $\mu_{\rm HEMT}$, $\mu_{\rm MESFET}$, and $\delta n_{\rm HEMT}$ mean carrier mobility in the InGaAs channel, that in the AlGaAs layer, and saturated carrier density in the InGaAs channel, respectively [11]. $P_{\rm opt,sat}$ and $\delta n_{\rm HEMT,max}$ represent optical power and maximum excess carrier in the InGaAs channel at the onset of parallel conduction.

The photovoltaic effect, which is a result of the accommodation of optical excitation with a depletion of majority carriers at the heterojunction interface, appears mainly on the intrinsic and parasitic capacitances. Considering the optical absorption and excess carrier generation processes in PHEMT, $P_{\rm opt}$-dependent gate capacitance can be modeled as [10], [11]

$$C_g = C_{\rm go} + C_{\rm gp} \cong C_{\rm go}(1 + \xi' \sqrt{1 + \alpha' P_{\rm opt}}) \qquad (4)$$

with a $P_{\rm opt}$-dependent gate capacitance $C_{\rm gp}$, a structure-dependent parameter $\xi'$, and a structure/bias-dependent factor $\alpha'$ [12]. Under low optical stimulation, as a result, the optically induced gate capacitance linearly increases with $P_{\rm opt}$ in addition to the electrically controlled capacitance under $P_{\rm opt} = 0$.

$P_{\rm opt}$-dependent $f_T$ is shown in Fig. 3 as a function of $P_{\rm opt}$, $V_{\rm GS}$, and $V_{\rm DS}$. Under low optical power, $f_T - (P_{\rm opt}, V_{\rm GS}, V_{\rm DS})$ curve looks very similar to $g_m - (P_{\rm opt}, V_{\rm GS}, V_{\rm DS})$ curve. One of main causes to the variation of $f_T$ on $P_{\rm opt}$ is an increased transconductance (photoconductive effect) until the photo-induced gate capacitance (photovoltaic effect) plays a dominant role in $f_T$. Regarding the photoconductive effect on the $f_T$, the parasitic $Al_{0.3}Ga_{0.7}As$ MESFET, which is known as *a parallel conduction*, is also believed to play a deterministic role in $f_T$. Under $P_{\rm opt} \leq 3$ mW, the $In_{0.13}Ga_{0.87}As$ channel layer is predominant over the optically induced parasitic MESFET [9]. As a result, the total transconductance is governed by the conduction of $In_{0.13}Ga_{0.87}As$ channel PHEMT. However, the parasitic gate-to-source capacitance $C_{\rm gs}$ doesn't increase so much with $P_{\rm opt} \leq 20$ mW. This agrees well with experimental observation for $f_T - (P_{\rm opt}, V_{\rm GS}, V_{\rm DS})$ because the shape of the $f_T - (P_{\rm opt}, V_{\rm GS}, V_{\rm DS})$ curves is similar to $g_m - (P_{\rm opt}, V_{\rm GS}, V_{\rm DS})$ curve. Contrary to the $g_m - (P_{\rm opt}, V_{\rm GS}, V_{\rm DS})$, which was nearly saturated over $P_{\rm opt} \geq 3$ mW, $f_T - (P_{\rm opt}, V_{\rm GS}, V_{\rm DS})$ curve increases up to $P_{\rm opt} \geq 20$ mW.

Under high optical stimulation with $P_{\rm opt} > 3$ mW, on the other hand, we observed a saturation of $g_m$ resulting in the saturation of $f_T$ with $P_{\rm opt} \geq 20$ mW. This is partially due to the $g_m$ in the saturation region caused by the parallel conduction via the parasitic MESFET with an increased optical power [10], [11]. Although the saturated transconductance does not increase with an additional optical power, the $In_{0.13}Ga_{0.87}As$ channel layer (with a high transconductance) plays a dominant role. So, $f_T$ still increases with elevated optical power up to $P_{\rm opt} \cong 20$ mW. However, the gate capacitance $C_g$ increases with increasing $P_{\rm opt}$ due to a reduced depletion region with an elevated photovoltage under $P_{\rm opt} \geq 20$ mW, which agrees well with previously reported $g_m$ and $f_T$ characteristics [5]. For a given $P_{\rm opt}$, maximum values of $f_T$ are obtained at a small negative $V_{\rm GS}$ in the saturation mode, which has a saturated maximum drain current over all optical inputs and a small gate capacitance due to the pinched gate-drain capacitance.

$$g_m = \begin{cases} g_{\rm mo} + a\mu_{\rm HEMT} P_{\rm opt} + b\mu_{\rm MESFET} P_{\rm opt}; & P_{\rm opt} \leq P_{\rm opt,sat} \\ g_{\rm mo} + a'\mu_{\rm HEMT}\delta n_{\rm HEMT,max} + b\mu_{\rm MESFET} P_{\rm opt}; & P_{\rm opt} > P_{\rm opt,sat} \end{cases} \qquad (3)$$

Maximum frequencies of oscillation are shown in Fig. 4 as a function of $P_{\rm opt}$, $V_{\rm GS}$, and $V_{\rm DS}$. $f_{\rm max(MAG)}$ increases significantly with increasing $P_{\rm opt}$, especially at small negative $V_{\rm GS}$ and large $V_{\rm DS}$. $f_{\rm max(MAG)}$ increases almost linearly with $P_{\rm opt}$ for given $V_{\rm DS}$ and $V_{\rm GS}$. The shape of $f_{\rm max(MAG)} - V_{\rm DS}$ curves looks similar to $g_m - V_{\rm DS}$ curves at near pinch-off condition over all $P_{\rm opt}$. However, it is quite different from the shape of $g_m - V_{\rm DS}$ curves at small negative $V_{\rm GS}$. $f_{\rm max(MAG)}$ increases monotonically for $P_{\rm opt} \geq 3$ mW even though maximum values of $f_T$ change little over $P_{\rm opt} \geq 20$ mW for a specific $V_{\rm GS}$ and $V_{\rm DS}$. In addition, $f_{\rm max(MAG)} - (V_{\rm GS}, V_{\rm DS})$ characteristics for a specific $P_{\rm opt}$ shows significantly different shape from $(f_T - V_{\rm GS}, V_{\rm DS})$ curves as shown in Fig. 3, which has the same shape as $g_m - (V_{\rm GS}, V_{\rm DS})$ curves predominantly being controlled by $g_m$. As shown in Fig. 4, $f_{\rm max(MAG)}$ decreases sharply with negative $V_{\rm GS}$ at high optical stimulation while it is relatively less dependent on $V_{\rm GS}$ under low optical power. $f_{\rm max} - V_{\rm DS}$ curves look very similar to $g_m - V_{\rm DS}$ curve under large negative $V_{\rm GS}$ over all $P_{\rm opt}$. This implies that the dominant limiting factor in $f_{\rm max(MAG)}$ is $g_m$ under large negative $V_{\rm GS}$ for a given $P_{\rm opt}$. Under small negative $V_{\rm GS}$, on the other hand, $f_{\rm max(MAG)}$ sharply increases with increasing $V_{\rm DS}$ for given $V_{\rm GS}$ and $P_{\rm opt}$. This is believed to be mainly due to reduced total gate capacitance by the decreased $C_{\rm gd}$ with expanded pinch-off region deep into the channel from the drain for given $P_{\rm opt}$ and $V_{\rm GS}$ because $f_T$ is almost saturated at high $V_{\rm DS}$ for all $V_{\rm GS}$ and $P_{\rm opt}$.

## III. Conclusion

Microwave characteristics of an n-channel $Al_{0.3}Ga_{0.87}As/GaAs/In_{0.13}Ga_{0.87}As$ PHEMT under electro-optical stimulations are reported for possible applications as a photonic-microwave device and as a novel characterization technique for traps and interface states in hetero-interfaces. The current gain cut-off frequency strongly depended on both $V_{\rm GS}$ and $V_{\rm DS}$. Maximum frequencies of oscillation obtained from the maximum available power gain showed maximum values at fixed $V_{\rm GS}$ and $V_{\rm DS}$ over all optical power range. Under low $P_{\rm opt}$, microwave characteristics were mainly controlled by the transconductance while they are limited by the the gate capacitance and a parasitic MESFET parallel to the $In_{0.13}Ga_{0.87}As$ channel PHEMT under high optical power. In the extended small-signal photonic-microwave model, optically induced characteristic parameters were included for better description of PHEMT's under electro-optical stimulation.

## References


[1] R. Simons, *Optical Control of Microwave Devices*. Boston, MA: Artech House, 1990.

[2] A. A. de Salles, "$Al_{0.3}Ga_{0.7}As$/GaAs HEMT's under optical illumination," *IEEE Trans. Microwave Theory Tech.*, vol. 39, pp. 2010–2017, Dec. 1991.

[3] M. Z. Martin *et al.*, "High-speed optical response of pseudomorphic InGaAs high electron mobility transistors," *IEEE Photon. Technol. Lett.*, vol. 4, pp. 1012–1014, Sept. 1992.

[4] H. Mitra, B. B. Pal, S. Singh, and R. U. Khan, "Optical effect in InAlAs/InGaAs/InP MODFET," *IEEE Trans. Electron Devices*, vol. 45, pp. 68–77, Jan. 1998.

[5] S. H. Song *et al.*, "Photonic microwave characteristics and modeling of an $Al_{0.3}Ga_{0.7}As/GaAs/In_{0.13}Ga_{0.87}As$ double heterostructure pesudomorphic HEMT," *IEEE Microwave Guided Wave Lett.*, vol. 8, pp. 35–37, Jan. 1998.

[6] K. Lee, M. S. Shur, T. J. Drummond, and H. Morkoc, "Parasitic MESFET in (Al,Ga)As/GaAs modulation doped FET's and MODFET characterization," *IEEE Trans. Electron Devices*, vol. ED-31, pp. 29–35, Jan. 1984.

[7] M. A. Romero and P. R. Herczfeld, "Negative photoresponse in modulation doped field effect transistors (MODFET's): Theory and experiment," *IEEE Trans. Microwave Theory Tech.*, vol. 43, pp. 511–517, Mar. 1995.

[8] M. A. Romero, M. A. G. Martinez, and P. R. Herczfeld, "An analytical model for the photodetection mechanisms in high-electron mobility transistors," *IEEE Trans. Microwave Theory Tech.*, vol. 44, pp. 2279–2287, Dec. 1996.

[9] D. K. Schroder, *Semiconductor Material and Device Characterization*. New York: Wiley, 1998. (see p. 359 for photoemission measurement technique.).

[10] D. M. Kim, S. H. Song, H. J. Kim, and K. N. Kang, "Electrical characteristics of an optically controlled $N$-channel AlGaAs/GaAs/InGaAs pseudomorphic HEMT," *IEEE Electron Device Lett.*, vol. 20, pp. 73–76, Feb. 1998.

[11] D. M. Kim, G. M. Lim, and H. J. Kim, "Parallel conduction and nonlinear optoelectronic response of an $n$-channel pseudomorphic high electron mobility transistor," *Solid-State Electron.*, vol. 43, pp. 943–951, May 1999.

[12] P. J. Tasker and B. Hughes, "Importance of source and drain resistance to the maximum $f_T$ of millimeter-wave MODFET's," *IEEE Electron Device Lett.*, vol. 10, pp. 291–293, July 1989.

[13] M. B. Das, "A high aspect ratio design approach to millimeter-wave HEMT structures," *IEEE Trans. Electron Devices*, vol. ED-32, pp. 11–17, Jan. 1985.